

Attention-based Memory video portrait matting

Shufeng Song*

^a Nanyang Technological University, 50 Nanyang Ave, Singapore 639798

* e-mail: SHUFENG001@e.ntu.edu.sg

Abstract— We proposed a novel trimap-free video matting method based on the attention mechanism. By the nature of the problem, most existing approaches use either multiple computational expansive modules or complex algorithms to exploit temporal information fully. We designed a temporal aggregation module to compute the temporal coherence between the current frame and its two previous frames. Moreover, we also provided direct supervision for the temporal aggregation model to further boost the network’s robustness. We validated our method on various testing datasets and reached state-of-the-art alpha and foreground prediction results with a low network computation complexity(9.69 GMACs for 512*512 resolution images).

Keywords: trimap-free matting, attention mechanism, temporal similarity, direct supervision

1. INTRODUCTION

Matting focus on using input images to generate prediction alpha and foreground with rich details. Due to its variety of applications, such as using virtual backgrounds to protect personal privacy in online meetings and editing video backgrounds for film production, matting has become a hot topic in the computer vision area.

Assuming α , F and B denote image alpha, foreground, and background, respectively. Then we can tackle the matting problem by replacing the original background B with target background B' in one linear formula:

$$I = \alpha F + (1 - \alpha)B' \quad (1)$$

Most matting algorithms usually expected a pre-annotated trimap for each frame in the training dataset to better separate an image into alpha, foreground and unknown region[18, 30, 22]. However, manually labelling the mixed pixels occupied by alpha and foreground, which belong to the trimaps’ unknown region, is impractical, especially when holes and transparent areas exist in the boundary of the matting objects[32]. Consequently, the quality of the manually annotated trimaps and the amount of dataset available are two constraints of those algorithms.

To minimise the limited precision and scale of existing trimap matting datasets, some latest work attempts to optimise the input trimap quality via trimap adaption module[6] or leverage the STM-based trimaps method to generate integral trimaps by putting several keyframes’ trimaps as input[34]. Moreover, Lin *et al.* proposed Real-time high-resolution background matting[16] which puts pre-captured backgrounds as auxiliary matting input and yields excellent quality when the backgrounds images are adequately offered. Similar idea are used by Soumyadip *et al.*[26]. However, it fails to deal with commonly seen dynamic backgrounds problems and using extra RGB backgrounds as input almost doubled the network parameters size.

Video matting is closely related to image matting in that each frame of the matting output essentially solves the corresponding video matting problem. Some video matting algorithms have reached a relatively good result on alpha and foreground prediction by processing video sequential frame-by-frame [16, 38, 26], despite ignoring the temporal coherence among consecutive frames. Then experiments show that fully exploiting the temporal information may improve the matting performance for several reasons. First, because the model can view successive frames and then make predictions, it can predict more coherent results and minimises flicker significantly. Second, temporal information can increase matting resilience in circumstances where an individual frame is uncertain. Third, temporal data allows the network to understand the background better over time [25]. Therefore, constructing new temporal-guided modules has become a hot topic to boost prediction accuracy.

This paper proposed a trimaps-free attention-guided video matting framework to exploit the temporal information. Semantic segmentation is also added to the training progress to increase the network robustness. The main contribution can be summarised as follows:

- (1) First, an attention-based module is introduced to memory the cues of the previous two video frames and propagated to the current frame to enhance the temporal coherence.
- (2) Direct supervision of the attention-based module is provided by interpolating the ground truth alpha and foreground to the same shape of the feature map.
- (3) Finally, we collected and aggregated primary open-source datasets for training.

2. Related Work

2.1. Image segmentation

Image segmentation aims to divide an image into regions corresponding to different objects on pixels level, which could be used to separate the portrait boundary mask from the image background. State-of-the-art segmentation structure such as Atrous-Spatial-Pyramid-Pooling(ASPP) from DeepLabV3[2] has been used to help locate human subjects in matting program[16, 25]. Ke *et al.* have also modified the ASPP to lower computational overhead without decreasing the performance[19]. Our method follows the track of previous work and combines ASPP with the attention-based memory module to complete the encoding operation.

2.2. Attention mechanism

In short, the attention mechanism maps a query and key-value pairs to an output sum of weighted values. While weighted values are determined by their scaled-dot-product between corresponding query and keys[1]. This approach has been widely used in the segmentation area to adjust network weights dynamically[36, 37, 39]. Moreover, experiments also demonstrate fusing feature maps from successive frames via attention mechanism may improve temporal consistency[23, 31].

2.3. Memory network

Determining cues from which frames are worth memorizing is the central problem of the memory network. Researchers commonly use the first[15, 10] or the previous one frame[27, 11, 5] as reference. As shown in Fig. 1(a), the former structure propagates the information consecutively can handle changes well but also accelerate the spread of errors. On the other hand, the latter design in Fig. 1(b) is inefficient to extract the necessary temporal information. To take advantage of the former two approaches, we have to extend the idea of the memory network and compute the temporal coherence between the current frame and its two previous frames. Fig. 1(c) demonstrates our final memory network structure.

2.4. Temporal guided in video matting

Robust video matting[25] adopts the ConvGRU[20] module in the decoder at multiple scales to fully exploit the temporal information. Still, they could merely pass half of the channel to cut its computation cost through the module. Others present a complex algorithm to restore temporal backgrounds information via historical frames[14, 31]. To eliminate those issues, we propose a novel attention-based memory module with less computation complexity and reach the SOTA results.

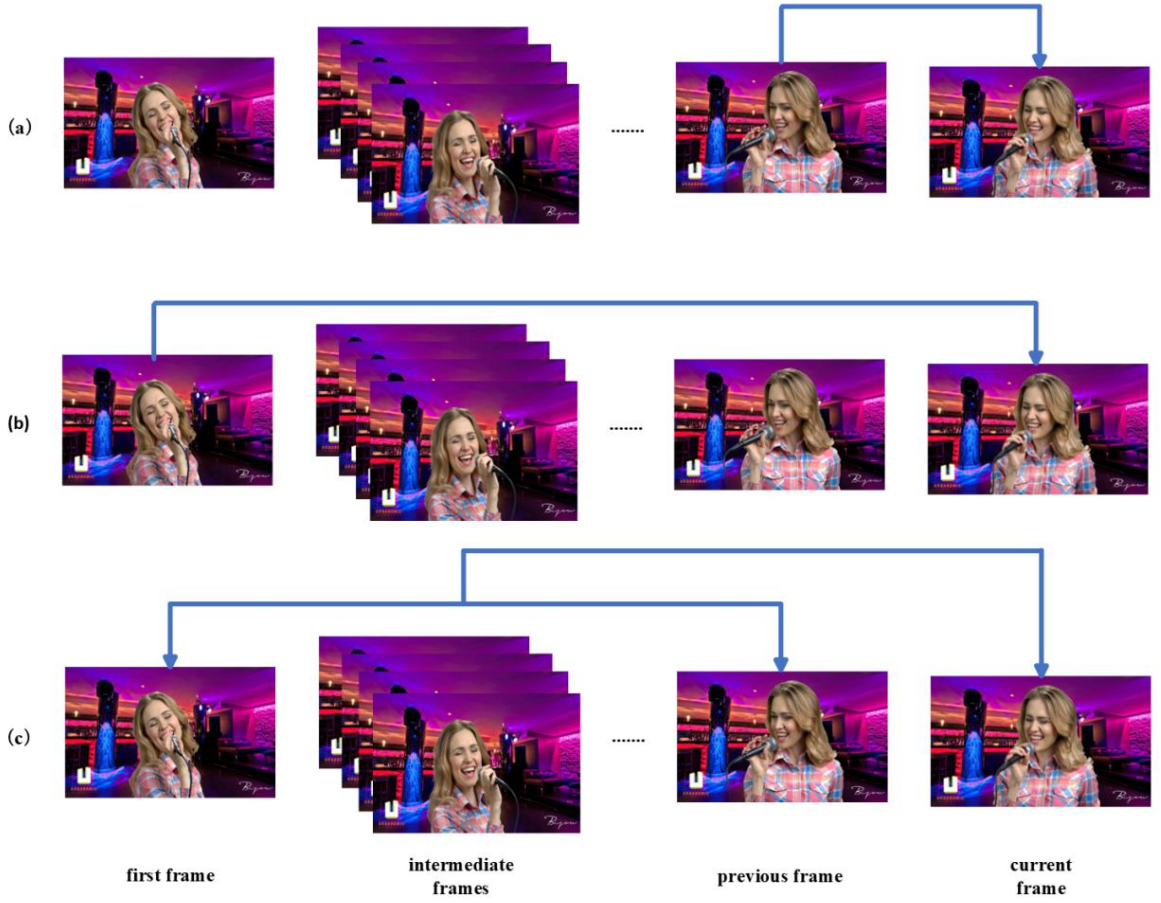


Figure 1: Different structures of memory network. (a)Using the previous frame as reference. (b)Using the first frame as reference. (c)The structure we adopted.

3. Model Architecture

Our approach is divided into four components that jointly address the video matting task and are trained end-to-end. MobileNetV3[9] is responsible for extracting feature maps from all frames as the backbone structure. Key-value pairs are then generated in the attention-based memory block by further encoding the feature maps to measure relative matching scores over spatial-temporal locations between memory and query frames. More specifically, keys are used to determine where to reconstruct relevant memory, and values store detailed information for the alpha, foreground prediction. Finally, the temporal-guided memory module reconstructs the new feature maps. It outputs a three-channel foreground and a one-channel alpha after multiple layers up-sampling blocks and one layer output block. The overall structure is shown in Fig 2. and implementation details of each block are illustrated as follows.

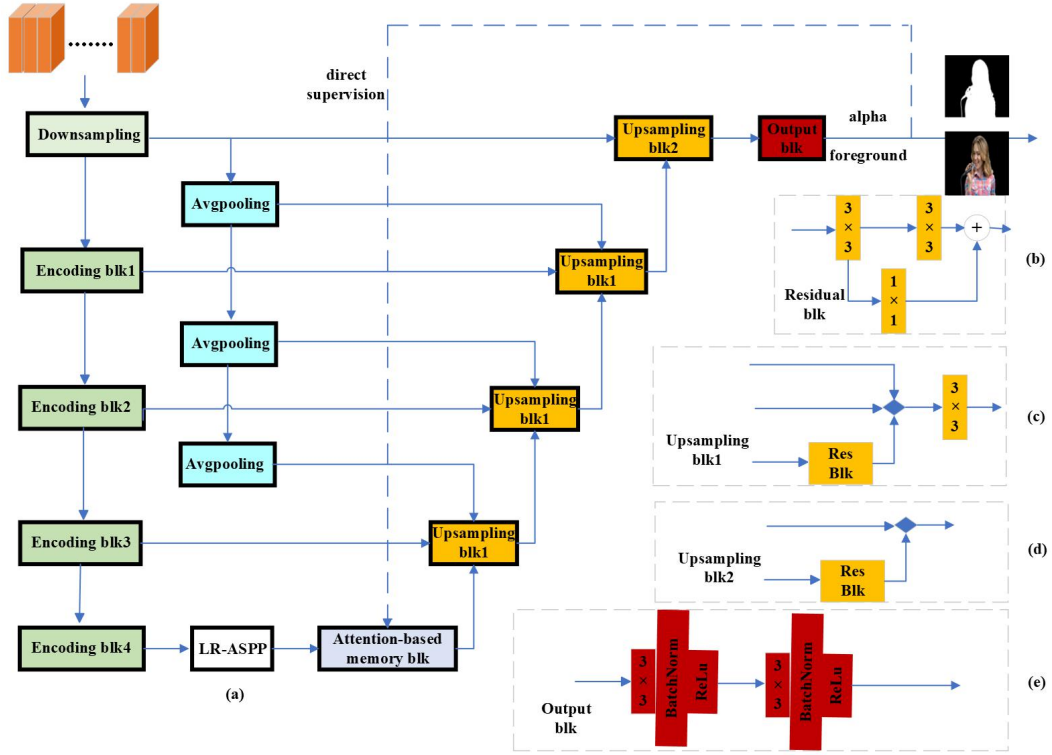


Figure 2: Overall structure of our matting network.

3.1. Backbone structure

MobileNetV3 pre-trained on ImageNet[24] is adopted as the default feature extraction network. Similar to most previous works, the 4th block of MobileNetV3 uses dilated convolution to preserve the feature map resolution from further down-sampling. Other complex structures such as ResNet50[8] can also be used to enhance the feature extraction quality. And eventually, feature maps at the resolution of $1/2$, $1/4$, $1/8$, and $1/16$ the down-sampled images are used for further processing.

3.2. Attention-based memory block

Key-value generator takes individual feature maps from each frame as input and outputs key-value pairs by passing through one convolution layer with Relu[21] activation function. Fig 3. (a) and Fig 3. (b) shows the detailed structure. Conv1 and Conv2 reduce the channel size to $1/8$ and $1/2$ to generate key and value, respectively. Therefore a feature key with the size of $[C/8, H/16, W/16]$ and a feature value with the size of $[C/2, H/16, W/16]$ are generated, where H and W denote down-sampled images' height and weight. C is the feature dimension of ASPP output.

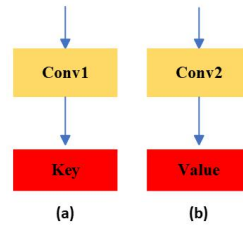


Figure 3: (a)Structure of key generator. (b)Structure of value generator.

Temporal-guided memory module: For the first two frames, our module in Fig 4. uses the frame itself as a reference and starts to memorize previous temporal information from the third frame in a video sequential. The inference and query frames are first encoded as key-value pairs via the key-value generator. Then a 4D key-memory K_m and value-memory V_m are embedded by concatenating the first and previous frames' key-value pairs into the same dimension (key-memory shape: $[2, C/8, H/16, W/16]$, value-memory shape: $[2, C/2, H/16, W/16]$). Finally, key-value pairs for memory and query go through the attention-based block and reconstruct the query frame feature map.

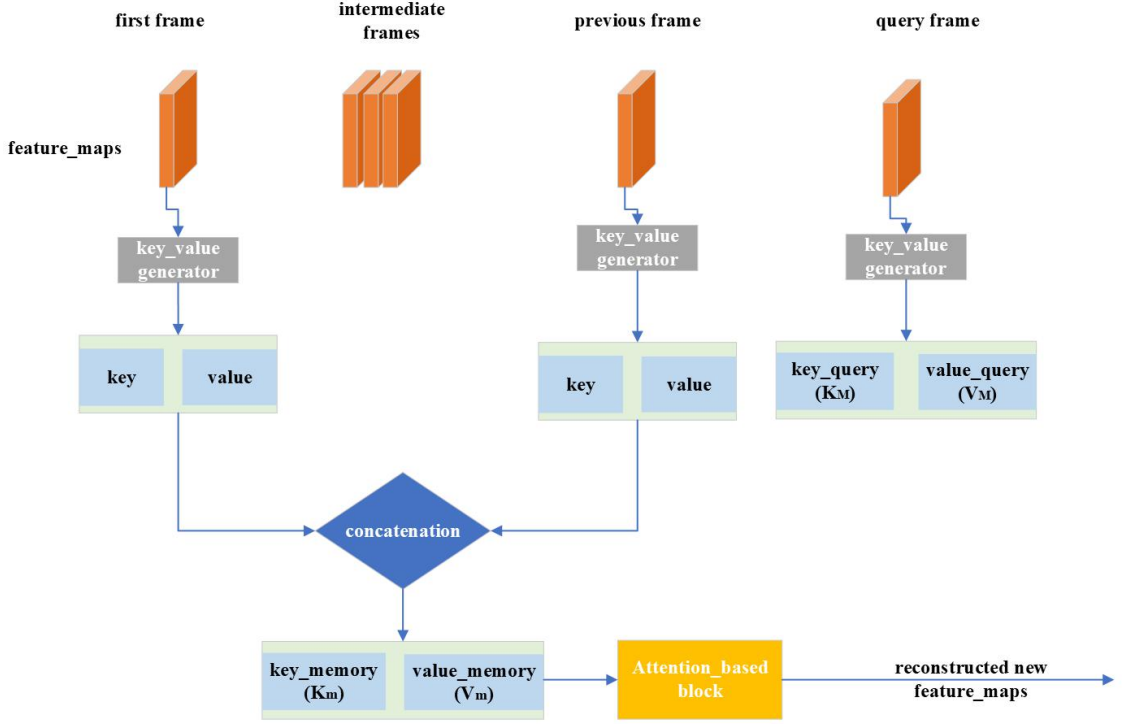


Figure 4: Overview of Temporal-guided memory module.

Attention-based block: Every pixel on key-value pairs for memory and query are well matched over the space-time location to generate corresponding weight matrix, which is used as a guideline to adjust the tensor value of value-memory V_M' in below [formula 2](#), where i and j are the index of the key-query and the key-memory location.

$$V_M' = \sum_j \text{softmax}(K_{m,i} \cdot K_{Q,j}) V_{m,j} = \sum_j \frac{\exp(K_{m,i} \cdot K_{Q,j})}{\sum_i \exp(K_{m,i} \cdot K_{Q,j})} V_{m,j} \quad (2)$$

Then the final feature map for each frame f could be retrieved by concatenating V_M' with original query-value V_Q . The formula is as follows, where $[,]$ represent concatenation function:

$$f = [V_M', V_Q] \quad (3)$$

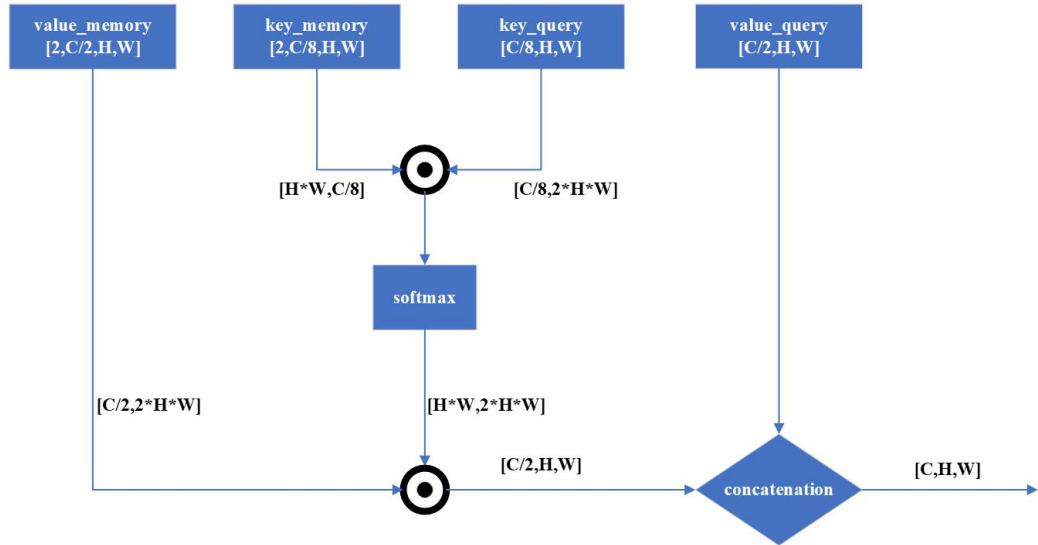


Figure 5: Detailed implementation of the attention-based block.

3.3. Up-sampling block

Up-sampling block operates at the scale of 1/16, 1/8, 1/4, and 1/2. [Fig 2.](#) demonstrates the detailed implementation of those Up-sampling blocks. Up-sampling block 1 in [Fig 2.\(b\)](#) repeats three times. First, it concatenates the bilinearly up-sampled output from the previous module with the same scale feature map and down-sampled images after multiple average-pooling layers. Then a

residual block is appended to reduce the channel number further and merge the feature maps. Up-sampled block 2 in Fig 2.(c) has a similar structure and function with Up-sampled block 1 but concatenates only previous output and down-sampled images before the output block.

3.4. Output block

Output block in Fig 2.(d) contains merely two 3×3 convolutional layers followed by Batch Normalization[12] and Relu[21] activation to downsized to 3 projection foreground channels and one alpha channel.

4. Matting dataset

Since most matting datasets' scale and quality limitations, we collect multiple images and video matting datasets to train our model. Following formula 1, we can generate a large set of training/validation/testing images by replacing the background of the compounded alpha and foreground images. The brief introductions of the datasets we use are listed as follows, and each matting dataset provides ground-truth foreground images and its corresponding alpha matte.

4.1. Image matting datasets

Aisegment is one of the most extensive human portrait matting datasets, with a total of 34427 images collected from Flickr, Baidu, and Taobao at a resolution of 600×800 . We randomly choose 75 percent of the images for training, 10 percent for validation, and 15 percent for testing. Despite its vast amount of data, the lack of fine boundaries such as hair contours in ground-truth alpha makes it only suitable for the first few training epochs, contributing to the convergence of network parameters.

Adobe image matting [19] is an object matting dataset. It provides 420/15/10 images of humans in the training/validation/testing data. Hence, we decide to merge it with Aisegment into a new image matting dataset and use it for image matting purposes.

4.2. Video matting datasets

VideoMatte240K collected by Lin *et al.*[16] consists of many facial and body motions and contains 484 unique images sequential at 4K and HD resolution. We randomly split those video clips into 474:5:5 for training, validation, and test mission.

VideoMatting108 constructed by Zhang *et al.*[34] is another video matting dataset with 108 foreground clips with corresponding ground-truth alpha matte at 1080p resolution. It also contains 109 clips of indoor and outdoor background image sequences, including camera movement, the passing of cars and pedestrians, and Illumination variation. We split 104:2:2 clips of matting date and 95:7:7 of background data clips for train, valid, and test. Therefore abundant RGB inputs with stationary and variable backgrounds can be compounded following formula 1. The first column in Fig 6. is an example of what our synthesized data looks like.

5. Training strategy

We followed the method of Robust video matting[25] by performing the training of semantic segmentation and matting simultaneously. On the one hand, the matting alpha is similar to the human-annotated binary mask. However, pooling and convolution operations in most segmentation tasks result in the insufficient accuracy of portrait boundary[13]. On the other hand, unlike most traditional matting algorithms in the introduction that provide trimaps or ground-truth backgrounds as an extra input, our method relies on segmentation to locate the human position and comprehend the scene semantically.

During the training process, a parameter T is added to control the length of input frames. For instance, $T=15$ indicates that the network will first take a sequence of 15 frames as input and extract the temporal-guided information of each frame in the attention-based memory block before passing

to the up-sampling layers. T depends on your GPU's memory size, and we try to maximize it to strengthen the network's handling compatibility of long sequences. We also cropped the input images size randomly and applied multiple data augmentation techniques, including flipping, rotation, scaling, saturation, contrast, hue, and color augmentation, to generalize the real-world situations.

5.1. Training Procedure

Image matting for stage 1: We train our model at the resolution of 512*512 on Aisegment and Adobe image matting combination dataset for five epochs. For image matting task, exploiting time coherence among multiple independent frames is unnecessary, so T are set to 1. As for the training hyper-parameters we set the learning rate equal to 1e-4 for the backbone structure and 2e-4 for the rest network.

Video matting for stage2: We maximize T to our GPUs' limitation and train 20 epochs each for VideoMatte and VideoMatting108 dataset. The images resolution decrease to 512*288 while the learning rate remain unchanged from stage 1. Our network can better learn the long-term dependencies of a long video sequence to handle the real-world problem in this training stage.

High-resolution video matting for stage3: Deep Guided filters [7] are integrated to the end of our network in stage 3 to efficiently generate the high-resolution projection outputs by giving its final hidden feature map and corresponding low-resolution alpha and foreground. We set $T=7$ and trained five epochs each for VideoMatte and VideoMatting108 dataset at 1920*1080 resolution. The learning rate of Deep Guided filters is 2e-4, and the rest of the network is reduced to 1e-5 for further learning.

5.2. Loss function

Image loss term L_{im} : The image loss term L_{im} only considers single frame prediction results, so we directly inherit loss function design from previous work. Specifically, it's a combination of alpha L1 loss L_α , alpha Laplacian loss L_{lap} [4], and composition loss L_{com} [33]. Assuming α_t, F_t is the ground-truth alpha matte and foreground, then α'_t, F'_t represent their projection values. L_{im} can be calculated as:

$$L_\alpha = ||\alpha_t - \alpha'_t||_1 \quad (4)$$

$$L_{lap} = \sum_s 2^{s-1} ||L_{pyr}(\alpha_t) - L_{pyr}(\alpha'_t)||_1 \quad (5)$$

$$L_{com} = ||\alpha_t F_t - \alpha'_t F'_t||_1 \quad (6)$$

$$L_{im} = L_\alpha + L_{lap} + L_{com} \quad (7)$$

Temporal loss term L_t : Drawn inspiration from the Context Prior for Scene Segmentation[35], we use the reconstructed feature map from attention-based memory block to generate low-dimension alpha α_t^{lr} and foreground F_t^{lr} for each frame and compute their L1 loss with the ground-truth alpha α_t^{lr} and foreground F_t^{lr} that been down-sampled to the same size, which provides direct supervision to the Attention-based memory block. We also calculate the temporal coherence loss L_{tem} [29] to further boost the learning process.

$$L_{tem-agg} = ||\alpha_t^{lr} - \alpha_t^{lr'}||_1 + ||F_t^{lr} - F_t^{lr'}||_1 \quad (8)$$

$$L_{tem} = ||\frac{d\alpha_t}{dt} - \frac{d\alpha_t'}{dt}||_2 + ||\frac{dF_t}{dt} - \frac{dF_t'}{dt}||_2 \quad (9)$$

$$L_t = L_{tem-agg} + L_{tem} \quad (10)$$

The overall loss function L_{vid} is a summation of above two different terms:

$$L_{vid} = L_{im} + L_t \quad (11)$$

6. Evaluation

Each sample in the Image-matting test dataset randomly picks a background test image to generate a synthesized image for benchmark use. And we also build video benchmark clips by composing each test sample from VideoMatte240K and VideoMatting108 onto fix backgrounds and backgrounds sequence. Each clip contains 50 frames with portrait and background movement.

Since the copyright of most matting datasets, previous works train and validate their models on their private datasets, making it unfair to evaluate the actual performance. In our experiment, we compare the performance of several state-of-the-art matting structures under a similar environment. To fairly compare with other trimap-free algorithms, we re-trained BGM[16] by inputting synthesizing RGB images and its first frame of the ground-truth background. For RVM[25], we followed the same training process and re-train it with our combined datasets. However, we had to change the maximum input length at one time to fit our device memory limitation. Noted that the source code of ModNet[38] hasn't been fully open-sourced yet, so we have to run our test data on their web demo for comparison.

6.1. Performance evaluation

Due to the property of matting tasks, we directly inherit some index values from segmentation tasks to evaluate the output results. Those index values including mean absolute difference (MAD), mean squared error (MSE), spatial gradient (Grad)[3], connectivity (Conn)[3], and dtSSD[17]. Table 1 shows the low-resolution benchmark results. The result indicates that BGM can only produce poor results with limited background information, and our method outperforms any trimap-free matting method. The lower MSE for alpha matte and foreground shows our model can generate accurate projection results. The value of dtSSD also demonstrates that the attention-based memory module in our model can fully exploit the temporal coherence. Then we run our model in 1080P, and the conclusion remains unchanged. Noted that ModNet doesn't generate foreground as its output.

Dataset	Method	Alpha					Foreground
		MAD	MSE	Grad	Conn	dtSSD	MSE
Image-matte 512*512	ModNet	12.391	6.854	7.463	1.864	4.456	
	BGM	21.897	17.640	3.784	2.874	4.987	19.284
	RVM	5.259	1.827	3.194	1.293	1.115	1.467
	Ours	4.702	1.288	2.047	1.084	0.934	1.113
VideoMatting108 512*288	ModNet	14.657	7.029	8.565	1.654	6.981	
	BGM	32.986	24.597	6.874	3.157	7.054	5.074
	RVM	6.248	3.399	2.718	0.878	3.820	4.709
	Ours	6.041	3.081	2.223	0.879	1.668	3.680
VideoMatte240K 512*288	ModNet	16.708	7.876	9.762	1.439	7.698	
	BGM	35.964	29.874	7.314	2.988	7.956	4.569
	RVM	6.816	1.316	1.238	0.529	3.530	7.055
	Ours	5.629	0.700	0.725	0.387	3.001	5.581

Table 1: Low resolution comparison between the results of four algorithms

Dataset	Method	Alpha				Foreground
		MAD	MSE	Grad	dtSSD	MSE
Image-matte 2048*2048	ModNet	10.048	4.894	12.512	3.081	
	RVM + DGF	5.797	2.328	17.502	1.343	1.089
	Ours +DGF	2.717	0.539	6.856	1.117	0.590
VideoMatting108 1920*1080	ModNet	13.823	6.789	21.469	2.197	
	RVM + DGF	7.769	4.887	12.531	1.852	4.796
	Ours +DGF	2.050	0.501	5.899	1.497	2.473
VideoMatte240K 1920*1080	ModNet	17.694	9.876	25.521	2.563	
	RVM + DGF	6.668	1.233	15.566	4.039	7.561
	Ours +DGF	4.011	0.287	3.569	2.014	6.913

Table 2: High resolution results comparison between three algorithms

In Fig. 6, from left to right, are the original input frames, alpha prediction from ModNet, RVM, and our approach. Compared with algorithms that use temporal information to process successive sequences, we can observe apparent flicker marked in the red box for ModNet. Moreover, our method can generate a clearer and smoother portrait boundary than RVM. The green box shows that the boundary of the human ear disappears in RVM, which often introduces artifacts such as residual of the original background in real-life matting applications. In summary, our method can store more boundary details and results in a better matting performance.

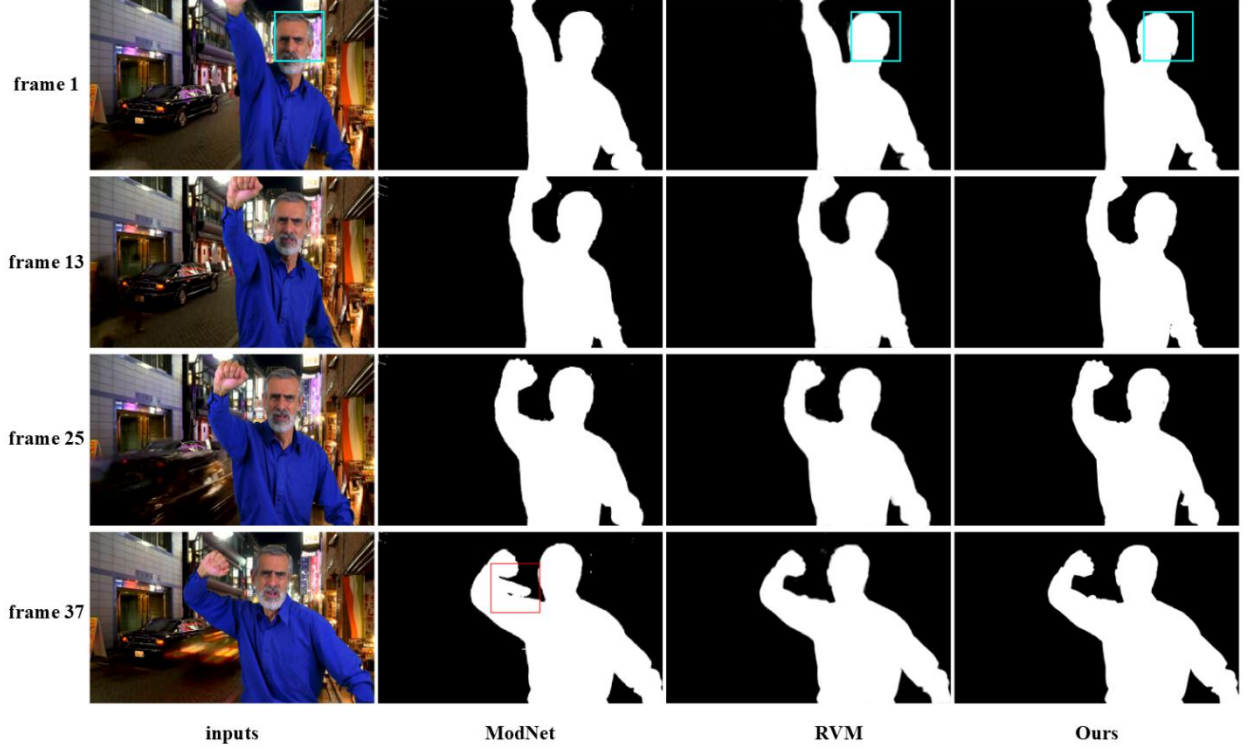


Figure 6: Display of original input and corresponding alpha projections.

6.2. size and computational complexity evaluation

Giga-Multiply-Accumulation-operations per-second[28] are used to evaluate the computational complexity of different networks. Table 3 shows that our structure is slightly more complex than RVM but is better than other methods. Noted that ModNet source code hasn't been fully open-sourced, so we can't calculate its computational complexity yet.

512*512	Parameters (Million)	Gmacs
ModNet	6.487	
BGM	4.99	15.04
RVM	3.75	8.11
ours	3.89	9.69

Table 3: size and computational complexity comparison between three algorithms

7. CONCLUSIONS

We proposed a novel trimap-free matting structure. First, an attention-based memory module was introduced, which significantly enhanced the network's ability to exploit temporal information for videos. Secondly, we used direct supervision to train the previous block and contribute to the network robustness. Our method performs the best among the existing methods in terms of projection accuracy. We believe the proposed attention-based memory module and its training strategy have a great potential to become breakthroughs in solving the video matting problems. In the future, we plan to do more experiments on multi-object matting and look forward to the applications of matting projects.

ACKNOWLEDGEMENTS

The author would like to express gratitude to Prof Lap-Pui Chau for his advice in model improvements.

CONFLICT OF INTERESTS

The process of writing and the content of the article does not give grounds for raising the issue of a conflict of interest".

COMPLIANCE WITH ETHICAL STANDARDS

This article is a completely original work of its authors; it has not been published before and will not be sent to other publications until the PRIA editorial board decides not to accept it for publication".

REFERENCES

- [1] Vaswani A, Shazeer N, Parmar N, et al. Attention is all you need[J]. Advances in neural information processing systems, 2017, 30.
- [2] Chen L C, Papandreou G, Schroff F, et al. Rethinking atrous convolution for semantic image segmentation[J]. arXiv preprint arXiv:1706.05587, 2017.
- [3] Rhemann C, Rother C, Wang J, et al. A perceptually motivated online benchmark for image matting[C]//2009 IEEE Conference on Computer Vision and Pattern Recognition. IEEE, 2009: 1826-1833.
- [4] Yu C, Wang J, Gao C, et al. Context prior for scene segmentation[C]//Proceedings of the IEEE/CVF Conference on Computer Vision and Pattern Recognition. 2020: 12416-12425.
- [5] Sergi Caelles, Kevis-Kokitsi Maninis, Jordi Pont-Tuset, Laura Leal-Taixe, Daniel Cremers, and Luc Van Gool. One- ' shot video object segmentation. In IEEE Conference on Computer Vision and Pattern Recognition (CVPR). IEEE, 2017.
- [6] Shaofan Cai, Xiaoshuai Zhang, Haoqiang Fan, Haibin Huang, Jiangyu Liu, Jiaming Liu, Jiaying Liu, Jue Wang, and Jian Sun. Disentangled image matting. In ICCV, 2019.
- [7] Wu H, Zheng S, Zhang J, et al. Fast end-to-end trainable guided filter[C]//Proceedings of the IEEE Conference on Computer Vision and Pattern Recognition. 2018: 1838-1847.
- [8] Kaiming He, X. Zhang, Shaoqing Ren, and Jian Sun. Deep residual learning for image recognition. 2016 IEEE Conference on Computer Vision and Pattern Recognition (CVPR), pages 770–778, 2016.
- [9] Andrew Howard, Mark Sandler, Grace Chu, Liang-Chieh Chen, Bo Chen, Mingxing Tan, Weijun Wang, Yukun Zhu, Ruoming Pang, Vijay Vasudevan, Quoc V. Le, and Hartwig Adam. Searching for mobilenetv3, 2019.
- [10] Yuan-Ting Hu, Jia-Bin Huang, and Alexander Schwing. Maskrnn: Instance level video object segmentation. In Advances in Neural Information Processing Systems, 2017.
- [11] Yuan-Ting Hu, Jia-Bin Huang, and Alexander Schwing. Videomatch: Matching based video object segmentation. In European Conference on Computer Vision (ECCV), 2018.
- [12] Sergey Ioffe and Christian Szegedy. Batch normalization: Accelerating deep network training by reducing internal covariate shift, 2015.
- [13] Ye J, Jing Y, Wang X, et al. Edge-sensitive human cutout with hierarchical granularity and loopy matting guidance[J]. IEEE Transactions on Image Processing, 2019, 29: 1177-1191.
- [14] Sun J, Ke Z, Zhang L, et al. MODNet-V: Improving Portrait Video Matting via Background Restoration[J]. arXiv preprint arXiv:2109.11818, 2021.
- [15] Ankit Kumar, Ozan Irsoy, Peter Ondruska, Mohit Iyyer, James Bradbury, Ishaan Gulrajani, Victor Zhong, Romain Paulus, and Richard Socher. Ask me anything: Dynamic memory networks for natural language processing. In International Conference on Machine Learning, pages 1378– 1387, 2016.
- [16] Shanchuan Lin, Andrey Ryabtsev, Soumyadip Sengupta, Brian L Curless, Steven M Seitz, and Ira Kemelmacher-Shlizerman. Real-time high-resolution background matting. In CVPR, pages 8762–8771, 2021.
- [17] Erofeev M, Gitman Y, Vatolin D S, et al. Perceptually Motivated Benchmark for Video Matting[C]//BMVC. 2015: 99.1-99.12.
- [18] Forte M, Pitié F. \$ F \$, \$ B \$, Alpha Matting[J]. arXiv preprint arXiv:2003.07711, 2020.

- [19] Xu N, Price B, Cohen S, et al. Deep image matting[C]//Proceedings of the IEEE conference on computer vision and pattern recognition. 2017: 2970-2979.
- [20] Ballas N, Yao L, Pal C, et al. Delving deeper into convolutional networks for learning video representations[J]. arXiv preprint arXiv:1511.06432, 2015.
- [21] Vinod Nair and Geoffrey E. Hinton. Rectified linear units improve restricted boltzmann machines. In ICML, 2010.
- [22] Juan O, Keriven R. Trimap segmentation for fast and user-friendly alpha matting[C]//International Workshop on Variational, Geometric, and Level Set Methods in Computer Vision. Springer, Berlin, Heidelberg, 2005: 186-197.
- [23] Seoung Wug Oh, Joon-Young Lee, Ning Xu, and Seon Joo Kim. 2019. Fast userguided video object segmentation by interaction-and-propagation networks. In Proceedings of the IEEE Conference on Computer Vision and Pattern Recognition. 5247–5256.
- [24] Olga Russakovsky, Jia Deng, Hao Su, Jonathan Krause, Sanjeev Satheesh, Sean Ma, Zhiheng Huang, Andrej Karpathy, Aditya Khosla, Michael S. Bernstein, Alexander C. Berg, and Fei-Fei Li. Imagenet large scale visual recognition challenge. International Journal of Computer Vision, 115(3):211–252, 2015.
- [25] Lin S, Yang L, Saleemi I, et al. Robust High-Resolution Video Matting with Temporal Guidance[C]//Proceedings of the IEEE/CVF Winter Conference on Applications of Computer Vision. 2022: 238-247.
- [26] Soumyadip Sengupta, Vivek Jayaram, Brian Curless, Steve Seitz, and Ira Kemelmacher-Shlizerman. Background matting: The world is your green screen. In Computer Vision and Pattern Recognition (CVPR), 2020.
- [27] Jae Shin Yoon, Francois Rameau, Junsik Kim, Seokju Lee, Seunghak Shin, and In So Kweon. Pixel-level matching for video object segmentation using convolutional neural networks. In IEEE International Conference on Computer Vision (ICCV), 2017.
- [28] Vladislav Sovrasov. flops-counter.pytorch.
- [29] Yanan Sun, Guanzhi Wang, Qiao Gu, Chi-Keung Tang, and Yu-Wing Tai. Deep video matting via spatio-temporal alignment and aggregation. In Proceedings of the IEEE Conference on Computer Vision and Pattern Recognition, 2021.
- [30] Gupta V, Raman S. Automatic trimap generation for image matting[C]//2016 International conference on signal and information processing (IConSIP). IEEE, 2016: 1-5.
- [31] Paul Voigtlaender, Yuning Chai, Florian Schroff, Hartwig Adam, Bastian Leibe, and Liang-Chieh Chen. 2019. FEELVOS: Fast End-To-End Embedding Learning for Video Object Segmentation. In IEEE Conf. Comput. Vis. Pattern Recog.
- [32] Jue Wang, Michael F Cohen, et al. Image and video matting: a survey. Foundations and Trends? in Computer Graphics and Vision, 3(2):97–175, 2008.
- [33] Ning Xu, Brian L Price, Scott Cohen, and Thomas S Huang. 2017. Deep Image Matting. In IEEE Conf. Comput. Vis. Pattern Recog., Vol. 2. 4.
- [34] Zhang Y, Wang C, Cui M, et al. Attention-guided Temporally Coherent Video Object Matting[C]//Proceedings of the 29th ACM International Conference on Multimedia. 2021: 5128-5137.
- [35] Changqian Yu, Jingbo Wang, Changxin Gao, Gang Yu, Chunhua Shen, and Nong Sang. 2020. Context Prior for Scene Segmentation. In IEEE Conf. Comput. Vis. Pattern Recog. 12416–12425.
- [36] Changqian Yu, Jingbo Wang, Chao Peng, Changxin Gao, Gang Yu, and Nong Sang. 2018. Bisenet: Bilateral segmentation network for real-time semantic segmentation. In Eur. Conf. Comput. Vis. 325–341.
- [37] Changqian Yu, Jingbo Wang, Chao Peng, Changxin Gao, Gang Yu, and Nong Sang. 2018. Learning a discriminative feature network for semantic segmentation. In IEEE Conf. Comput. Vis. Pattern Recog. 1857–1866.
- [38] Ke, Z., Li, K., Zhou, Y., Wu, Q., Mao, X., Yan, Q., & Lau, R. W. (2020). Is a green screen really necessary for real-time portrait matting?. arXiv preprint arXiv:2011.11961.
- [39] Hang Zhang, Kristin Dana, Jianping Shi, Zhongyue Zhang, Xiaogang Wang, Amrith Tyagi, and Amit Agrawal. 2018. Context encoding for semantic segmentation. In IEEE Conf. Comput. Vis. Pattern Recog. 7151–7160.

Authors profile



Shufeng Song earned his bachelor degree from Beijing University of Posts and Telecommunications (2019). Presently, he is a M.Eng student in Nanyang Technological University. His current areas of interest include image segmentation and quantum machine learning.